Calibration of atmospheric effects on SAR interferograms by GPS and local atmosphere models: first results

Alessandro Bonforte [(1)], Alessandro Ferretti [(2)], Claudio Prati [(2)],
Giuseppe Puglisi [(1)], Fabio Rocca [(2)]

1 - Istituto Internazionale di Vulcanologia - CNR, Piazza Roma, 2, I-95123, Catania, Italy
2 - Dipartimento di Elettronica e Informazione - Politecnico di Milano, Piazza Leonardo da Vinci 32, I-20133, Milano, Italy

Journal of Atmospheric and Terrestrial Physics

Abstract

A comparison between the ZPD (Zenith Path Delay), obtained from GPS measurements, and the expected delay, derived from models used to compensate tropospheric effects on SAR interferograms, is made. The results of the two methods are comparable, though the available data set is not large enough for a complete statistical validation of the methods. The results of this preliminary study suggest a possible integration of GPS-based ZPD data with cheap and standard meteorological data, since the estimated atmospheric component proved to be similar. Furthermore, the impact on volcanology of the effects measured by GPS, and in particular on the determination of the depth of the volcanic sources, is discussed.

Introduction

Mt. Etna has often been used as a test site of new approaches for ground deformation studies in volcanic areas based on the use of satellites; such is the case, for instance, of the GPS, in the late 80's (Briole et al., 1992; Nunnari & Puglisi, 1994a; Nunnari & Puglisi, 1994b), and more recently of Differential SAR Interferometry (Massonnet et al., 1995; Briole et al., 1997; Lanari et al., 1998). Due to both its altitude (ranging from sea level up to 3300 m) and its climatic conditions one problem common to the two above mentioned applications is the atmospheric effect on the measurements. The experience carried out in more than ten years of GPS surveys on Mt. Etna allows to minimise these effects by carefully planning the campaigns (Puglisi et al., 1998), but how to address this problem in the DInSAR processing is still an open question.

The measurement of ground deformations with DInSAR is based on the comparison between two SAR images, acquired at different times (Massonnet & Rabaute, 1993). If on the surveyed areas a ground deformation phenomenon occurs between the two passes, the travel differences between the sensor and the ground in the two passes lead to a difference in the phase of the back-scattered radar wave. Based on this assumption the interferogram resulting from the comparison between the two images gives a picture of the ground deformation pattern, measured as displacement along the line of the sight of the sensor. Obviously these travel differences might be -partially or totally - also due to differences in the atmospheric properties between the two passes, and therefore the removal or the reduction of this unwelcome effect on the interferogram is a critical point in the DInSAR technique.

Recently, to overcome this problem approaches based both on the staking (Zebker et al., 1997) or on the calibration (Delacourt et al., 1997; Williams et al., 1998) are proposed. The former are based both on the availability of independent interferograms of the same area and on the assumption that no-deformation occurs between different stacked interferograms. This assumption, even though possible only in particular experimental conditions (e.g. for the 2 day-shift for the SIR-C interferogram set used by Zebker et al. (1997)), is not usual when the 35-day repeat cycle of ERS2 satellite is used to monitor active volcanic areas. Thus, approaches based on the calibration of DInSAR products using measurements carried out with independent sensors seem more suitable to routinely reduce the atmospheric effect.

If on a surveyed area a GPS geodetic network exists for ground deformation monitoring purposes the calibration might be performed using the Zenith Path Delay (ZPD) estimated by processing GPS data. Indeed, Williams et al. (1998) proposed a method that could greatly reduce the atmospheric noise in the DInSAR products by removing its long-wavelength components using the ZPD estimated by processing the GPS data. Furthermore, they discouraged the use of calibration method based on the use of ground-based meteorological data (Delacourt et al., 1997), because these data (and in particular the water vapour contents) cannot be suitably extrapolated along the microwaves path, according to experiments carried out on GPS data processing (Bevis et al., 1992). Although this drawback is somewhat true, it doesn't definitively close investigations about the use of ground-based meteorological data and how they could be integrated with GPS results. In fact the approach proposed by Williams et al. (1998) is strongly constrained by the GPS network configuration; sparse geometry prevents the reduction of short-wavelength components in the atmospheric noise. This limitation could be critical when short-wavelength ground deformations are investigated, such as those close to active craters (e.g. Pu'u O'o during 1994, Rosen et al., 1996). The possibility to integrate cheap ground-based meteorological data with "expensive" GPS results is probably the way to achieve a full removal of atmospheric noise in the DInSAR interferograms. To verify the congruence between the GPS-based ZPD and the result of calibration method based on ground meteorological data is the first step of this integration. This paper will address this problem.

GPS zenith delay observation

Since 1996 GPS measurements have been carried out, during the ERS-2 passes over Mt. Etna volcano; sometimes measurements have been carried out also during the ERS-1 passes. The aim of these measurements - carried out in the frame of an EC Project - was the estimation of the TEC (Total Electron Content) of the ionosphere and the ZPD (Zenith Path Delay) caused by the troposphere, in order to evaluate their effects for SAR interferograms creation. Four sites were chosen on Etna to carry out the measurements (Fig. 1, Table I): the *Istituto Internazionale di Vulcanologia* roof (IIV) in Catania, about 50 meters high above the sea level, the *Serra la Nave Astrophysics Observatory* (SLN) at about 1700 meters on the south-western flank, the *Etnean Volcanological Observatory* (EPDN) at about 2800 meters on the north-eastern side and, more recently, also the *Torre del Filosofo* (ETDF) station, at about 2900 meters on the southern side of the summit cone. This choice was made in order to obtain information at different altitudes and improve the tropospheric modelling. Snow coverage prevented carrying out measurements on the higher stations during the winter periods. In order to obtain better quality information about the ionosphere and troposphere, GPS data collected at Noto, Matera and Cagliari IERS sites were taken into account.

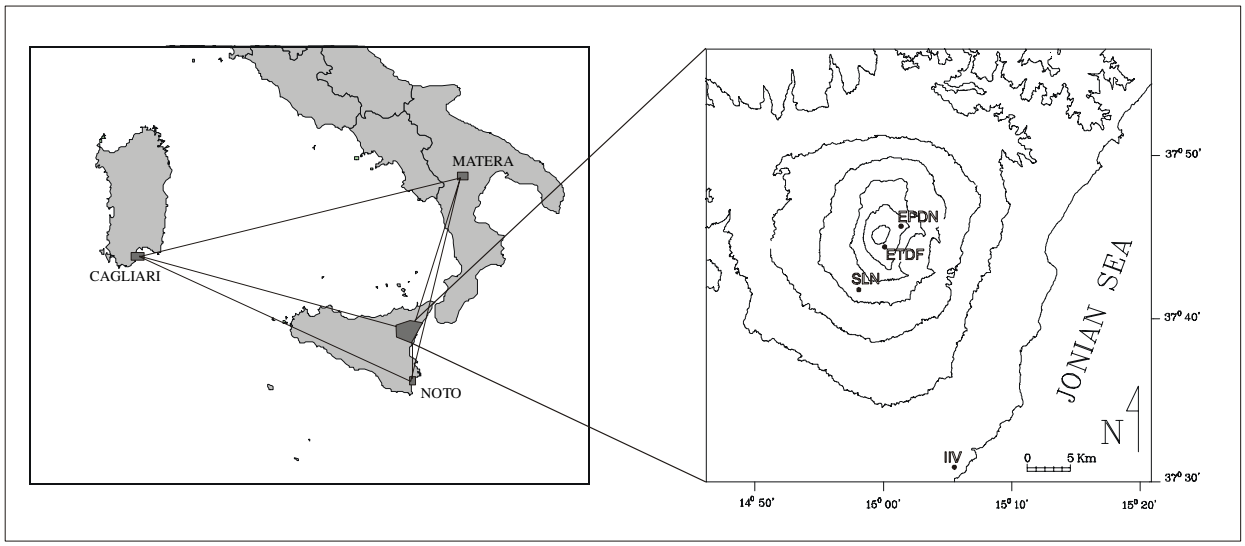

Figure 1. On the left, the geographic location of the investigated area, in southern Italy and the three ITRF stations considered in this work. On the right the Mt. Etna volcano and the GPS measurement sites are shown.

Each session was initially planned to last 4 hours, starting about two hours before and ending about two hours after the ERS-2 pass. Later on, longer sessions (6 hours) were adopted in order to overcome some ambiguity resolution problems occurring during the data processing, especially for the long baselines between the IERS stations or between them and the stations on the volcano. The relative short duration of the sessions was due, at the beginning of the experiment, to the limits of the suitable hardware; to maintain similar experimental conditions, the considered data set was selected not longer that 6 hours, even if, for instance, the receiver's RAM now used allows much more data to be saved. The data has been processed with Bernese 4.0 software developed at the Astronomical Institute of the University of Berne (Rothacher & Mervart, 1996).

The lowest part of the Earth's atmosphere consists in dry gases and water vapour, which is present only in the very first kilometres above the ground surface. These two components affect the signals differently and have different pressure profiles; the dry atmosphere is quite uniform in its distribution and constituents while the wet atmosphere varies widely both horizontally and vertically and with time.

The total effect of the troposphere on the GPS signals could be estimated resolving the well known phase double difference equation of the relative positioning between two stations (k and l) and two satellites (j and i), given by:

$$\phi_{Fkl}^{ij} = \phi_{Fk}^{i} - \phi_{Fk}^{j} - \phi_{Fl}^{i} + \phi_{Fl}^{j} = \rho_{kl}^{ij} + \lambda N_{Fkl}^{ij} - \beta_F I_{kl}^{ij} + \Delta\rho_{kl}^{ij} \qquad (1)$$

The βI^i_k and $\Delta\rho^i_k$ terms represent respectively the effects of the ionospheric and tropospheric refraction. This latter is given by:

$$\Delta\rho_k^i = \Delta\rho_{apr,k} f_{apr}\left(z_k^i\right) + \Delta\rho_k(t) f\left(z_k^i\right)$$

where:

$\Delta\rho_{apr}$ = Zenith Path Delay (ZPD) computed from tropospheric refraction models, function of (P, T, H), assumed a priori.

$\Delta\rho_k$ = Time-dependent ZPD Estimated in Least Squares Adjustment

$f_{apr}(z)$ = Mapping Function for a-priori model. It is a function of the zenith distance

$f(z)$ = Mapping Function used for parameter estimation. It is a function of the zenith distance and may be different from $f_{apr}(z)$.

The adopted software allows several tropospheric refraction models to be used, namely: Saastamoinen (1973), Hopfield modified (Goad & Goodman, 1974), Hopfield simplified (Wells, 1974) and Differential Refraction Model (Rothacher et al. 1986). The choice of a specific model is a task that will be addressed later on.

To overcome the effect of the ionosphere in the GPS solutions (and consequently also in the ZPD estimations) the *Iono-free* observable (L_3) was used. It is defined by the following equation (Beutler et al., 1989):

$$L_3 = \frac{1}{f_1^2 - f_2^2}\left(f_1^2 L_1 + f_2^2 L_2\right)$$

This observable makes it impossible to resolve the initial integer phase ambiguities (the λN term of the equation (1)), so the QIF (*Quasi Iono Free*) strategy, which resolves the ambiguities for the L1 and L2 frequencies separately, was adopted, as suggested by Rothacher & Mervart (1996). This kind of strategy requires a local ionosphere model that for each session was previously computed using both local and ITRF stations.

The final step of the processing was the troposphere parameters estimation for each station, using the *Differential Refraction Model*. This particular model computes the troposphere delay in the atmospheric layer between the lowest and the highest stations, using the Essen and Froome (1951) formulas, while for the troposphere delay above the highest station, the Saastamoinen (1973) model is applied. This choice was made after a trial period, during which the ZPD for each session and each station was computed using both the Saastamoinen model alone and the Differential Refraction Model. From the result of this first trial it was clear that the Differential Refraction Model solutions were affected by smaller errors than the Saastamoinen one. Since the behaviour of the troposphere delay variations, resulting from the two models, was similar, the model with the smallest error was adopted to carry out the following processing; in fact, large errors reflect significant misfit between the actual data and the adopted model.

Each GPS session has been divided into one-hour time windows and the ZPD was calculated for each of them. In the present work we consider the ZPD value relevant to the particular window that includes the time of the ERS pass: i.e. 09:00-10:00 UTC for descending passes and 21:00-22:00 UTC for ascending passes.

In order to investigate the suitability of the ZPD estimations, the next one-hour time window was also analysed for each session. Then the ZPD differences between the two windows are plotted. The plot reported in Fig. 2 shows that the variations of the ZPD during the same session are always less than 2 cm.

Furthermore, the largest differences are relevant to the daytime sessions (squares) probably due to large variations in the atmosphere conditions, more common during the day than in the night (triangles). As a consequence the measured variations of the ZPD and the relevant error bars seem suitable for the following analysis

GPS Sessions				ERS Passes		Stations			
#	Day	Start	End	Time	Orbit	IIV	SLN	OSV	TDF
269-96	25-09-96	19:15	23:15	21:16	07498	*	*	*	
276-96	02-10-96	07:40	11:40	09:41	07591	*	*		*
304-96	30-10-96	19:15	23:15	21:16	07999	*	*	*	
311-96	06-11-96	07:40	11:40	09:41	08092	*	*	*	
339-96	04-12-96	19:15	23:15	21:16	08500	*	*	n.r.	n.r.
346-96	11-12-96	07:40	11:40	09:41	08593	*	*	n.r.	n.r.
008-97	08-01-97	19:15	23:15	21:16	09001	*	*	n.r.	n.r.
015-97	15-01-97	07:40	11:40	09:41	09094	*	*	n.r.	n.r.
050-97	19-02-97	07:40	11:40	09:41	09595	*	r.f.	n.r.	n.r.
078-97	19-03-97	19:15	23:15	21:16	10003	*	*	n.r.	n.r.
120-97	30-04-97	07:40	11:40	09:41	10597	*	*	n.r.	n.r.
148-97	28-05-97	19:15	23:15	21:16	11005	*	*	n.r.	n.r.
155-97	04-06-97	07:40	11:40	09:41	11098	*	*		*
183-97	02-07-97	19:15	23:15	21:16	11506	*	*	*	
190-97	09-07-97	07:40	11:40	09:41	11599	*	r.f.	*	
218-97	06-08-97	19:15	23:15	21:16	12007	*	*	*	
225-97	13-08-97	07:40	11:40	09:41	12400	*	*	*	
253-97	10-09-97	19:15	23:15	21:16	12508	*	*	*	
260-97	17-09-97	07:40	11:40	09:41	12601	*	*	r.f.	
288-97	15-10-97	19:15	23:15	21:16	13009	*	*		
295-97	22-10-97	07:40	11:40	09:41	13102	*	*		
323-97	19-11-97	19:15	23:15	21:16	13510	*	*	n.r.	n.r.
330-97	26-11-97	07:40	11:40	09:41	13603	*	*	n.r.	n.r.
358-97	24-12-97	19:15	23:15	21:16	14001	*	*	n.r.	n.r.
365-97	31-12-97	07:40	11:40	09:41	14104	*	*	n.r.	n.r.
308-98	04-11-98	18:00	24:00	21:16	07498	*	*	*	
315-98	11-11-98	06:00	12:00	09:41	07591	*	*	*	
343-98	09-12-98	18:00	24:00	21:16	07999	*	*	n.r.	n.r.
350-98	16-12-98	06:00	12:00	09:41	08092	*	r.f.	n.r.	n.r.
013-99	13-01-99	18:00	24:00	21:16	19522	*	*	n.r.	n.r.
020-99	20-01-99	06:00	12:00	09:41	19615	*	*	n.r.	n.r.
048-99	17-02-99	18:00	24:00	21:16	20023	*	*	n.r.	n.r.
054-99	23-02-99	06:00	12:00	09:41	39789	*	*	n.r.	n.r.
055-99	24-02-99	06:00	12:00	09:41	20116	*	*	n.r.	n.r.
083-99	24-03-99	18:00	24:00	21:16	20524	*	*	n.r.	n.r.
089-99	30-03-99	06:00	12:00	09:41	40290	*	*	n.r.	n.r.
090-99	31-03-99	06:00	12:00	09:41	20617	*	*	n.r.	n.r.
117-99	27-04-99	18:00	24:00	21:16	40698	*	*		*
118-99	28-04-99	18:00	24:00	21:16	21025	*	*		*
124-99	04-05-99	06:00	12:00	09:41	40791	*	r.f.	*	*
125-99	05-05-99	06:00	12:00	09:41	21118	*	r.f.	*	*
152-99	01-06-99	18:00	24:00	21:16	41199	*	*	r.f.	*
153-99	02-06-99	18:00	24:00	21:16	21526	*	*	r.f.	*
159-99	08-06-99	06:00	12:00	09:41	41292	*	*		
160-99	09-06-99	06:00	12:00	09:41	21619	*	*	*	*
187-99	06-07-99	18:00	24:00	21:16	41700	*	*	*	*
188-99	07-07-99	18:00	24:00	21:16	22027	*	*	*	*
194-99	13-07-99	06:00	12:00	09:41	41793	*	*	*	*
195-99	14-07-99	06:00	12:00	09:41	22120	*	*	*	*

Table I. List of the GPS sessions and of the SAR passes over Mt. Etna during the considered experiment. Conventionally, the SAR orbits are distinguished in ascending (from South to North Pole) and descending (from North to South Pole). For the ascending passes the track and frame of the considered images are respectively 129 and 747, the time of the pass being 21:16 UTC, while for the descending passes the track and frame of are respectively 222 and 2853; the time of the pass is 09:41 UTC. In the last four columns, the asterisks indicate the occupation of the different GPS stations; n.r. = not reachable, for instance due to snow coverage problems, r.f. = receiver failures.

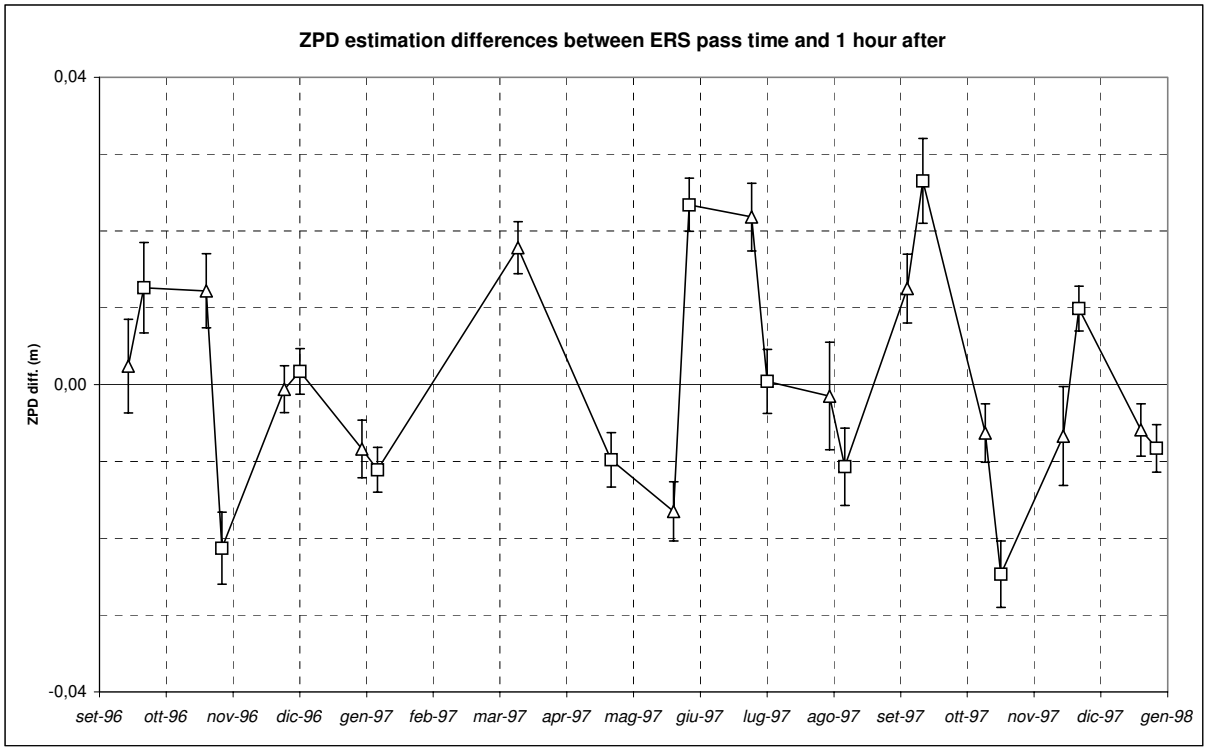

Figure 2

Once the main processing steps to evaluate the ZPD are established, the definitive fine tuning concerned the use of the data relevant to three ITRF stations, up to now used to determine both the ionosphere models and the IIV co-ordinates. Due the relative small duration of the measurement sessions carried out on the volcano, often ambiguity resolution problems have been encountered. In order to avoid this problem the final step of the processing was carried out excluding the three ITRF stations to avoid too long baseline computations between Mt Etna and ITRF stations. The ZPD was then calculated only for SLN, EPDN and ETDF, keeping IIV as a reference. This means that the ZPD variations measured at SLN, EPDN and ETDF stations have to be considered as relative to the IIV station, which is assumed stable.

The results of the processing of the sessions carried out during the experiment are plotted in the Figures from 3 to 6. These figures show that strong irregularities in the troposphere behaviour have been found, leading to ZPD variations of several centimetres. For the objectives of this work, we are interested in the relative variation of ZPD with respect to a reference time that, in the Figures from 4 to 6, is conventionally assumed as the sessions carried out respectively in 25/09/96, for the ascending passes, and in 2/10/96, for the descending. In the secondary ordinate axes of the Figures from 4 to 6 the number of interferogram fringes corresponding to the measured ZPD variations is reported. They are computed by the ratio $(2\ ZPD)/(\lambda \cos\theta)$, derived from Zebker at al. (1997), where, for the ESR1/2 SAR, λ=5.6 cm and θ=23°.

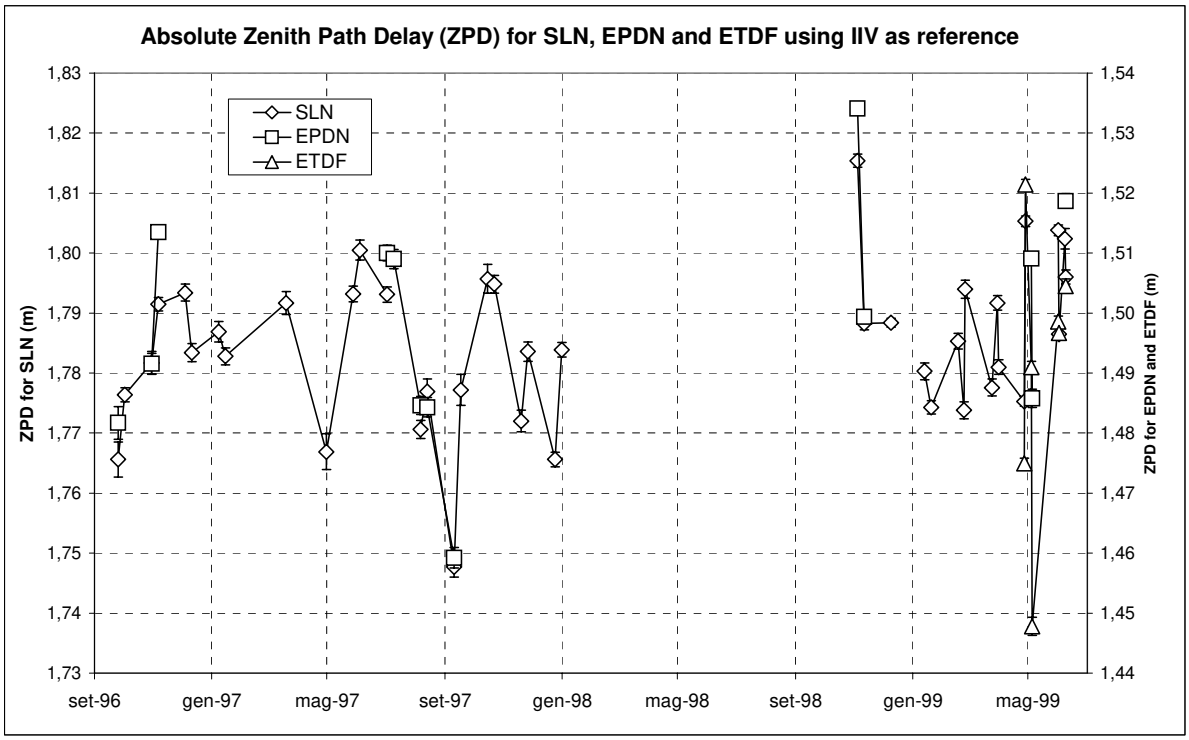

Figure 3

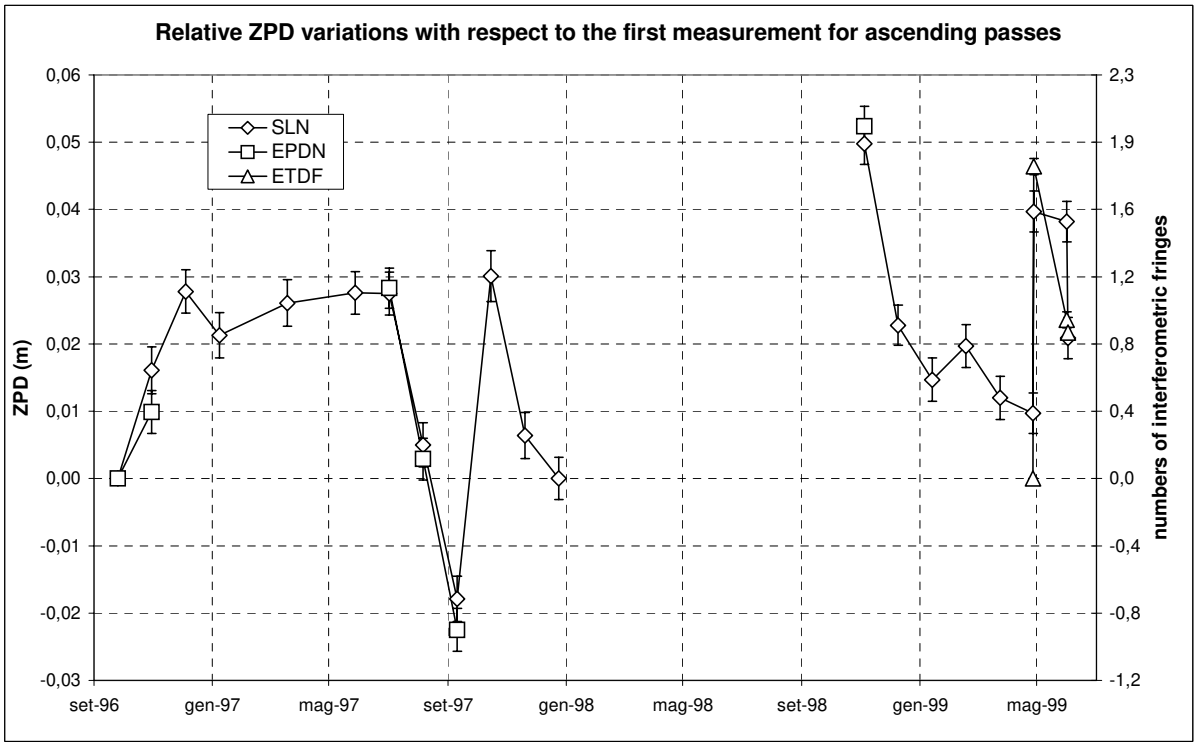

Figure 4

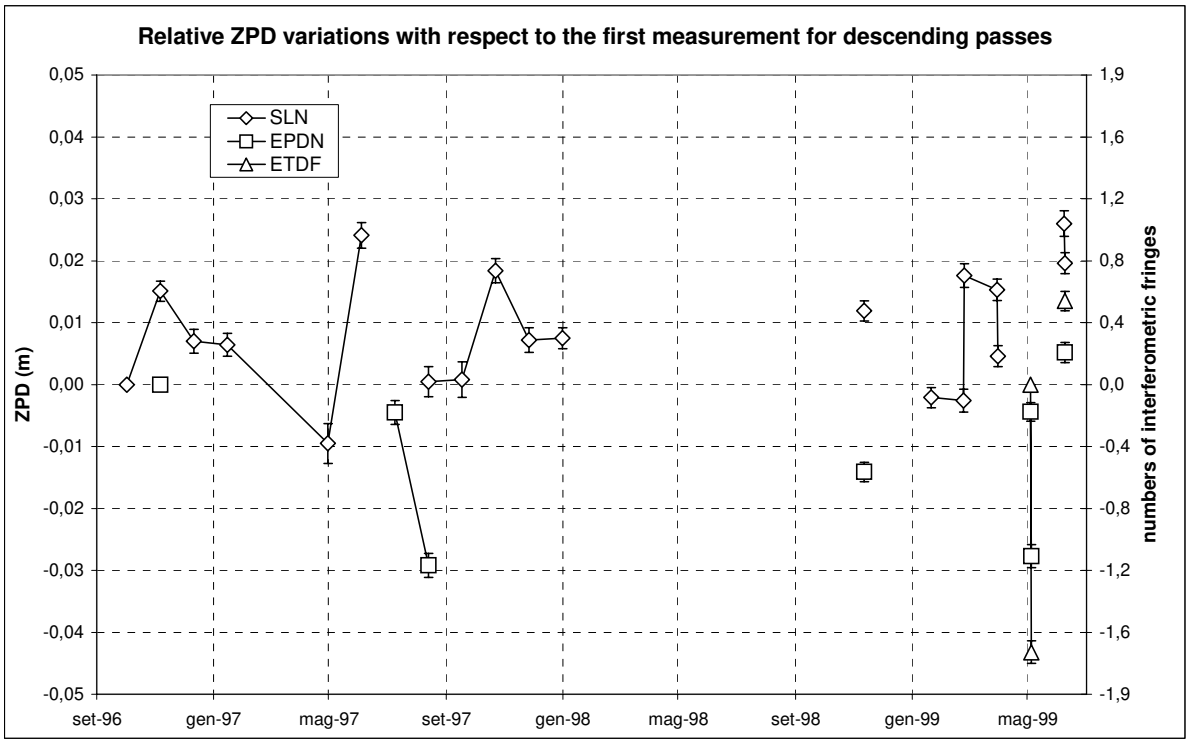

Figure 5

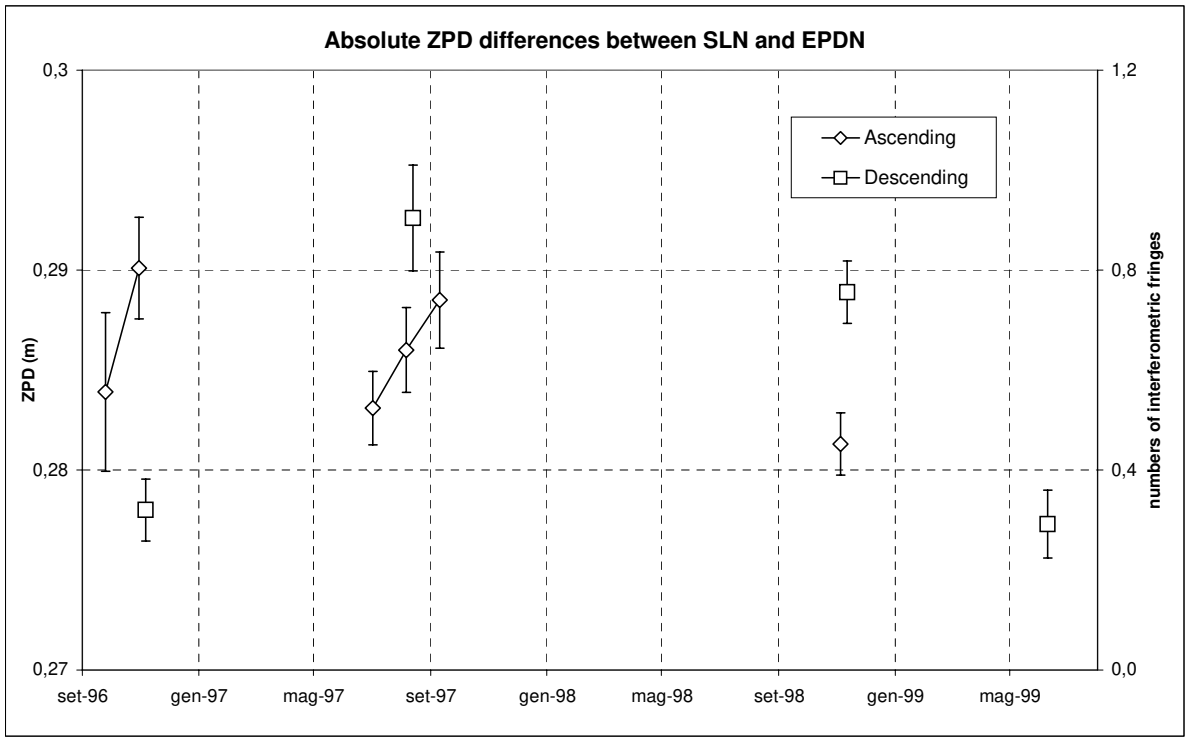

Figure 6

Discarding those absolute variations that affect the whole Etnean area uniformly (for the same reasons seen for the ionosphere), we can look at the differences between the stations, to have an idea how the troposphere variations can affect an interferogram. Figures 4 and 5 show strong differences in the troposphere behaviour between the IIV and SLN sites, leading to differences in ZPD variation up to 5 cm (7 cm in the worst case for ascending passes) between two ERS passes. Such differences are able to produce up to two fringes (or even more) on the lower flanks of Etna in the interferograms in the worst conditions,

simulating large scale inflation or deflation of the whole volcanic edifice. On the contrary, the troposphere seems to have a more homogeneous behaviour at higher altitude; in fact the variation of the ZPD difference between SLN and EPDN is limited to less than 1 cm for ascending passes and to little more than 1 cm for descending passes (Fig. 6). The same range of variation of the ZPD affects the troposphere between SLN and ETDF stations. However, it is remarkable that, between ETDF and EPDN sites the range of variations (0.004 ÷0.020 m) is comparable with those measured between SLN and the stations located at altitudes higher than 2800 m (Figure 6). Even if the data are very few to make more rigorous analysis, this last result is very important because it shows troposphere variations that are not totally dependent on the difference of altitude but also on small horizontal irregularities in the troposphere. A possible cause of the ZPD variation between the highest sites, which are close to the summit craters of the volcano, may be the different direction of the wind that drives the volcanic plume over one of the two stations. Unfortunately, the series of data are not complete for further investigations but this represents a stimulating start point for future studies.

SAR atmospheric delay modelling

The theory concerning atmospheric effects affecting ERS-1/2 SAR interferograms is similar to that used in GPS measurements, since both systems employ signals in the microwave band. As already pointed out, both ionospheric and tropospheric dishomogeneities affect the interferometric phase. The impact of TEC variations on SAR interferograms is usually limited, since the spatial extension of ionospheric effects corresponds to very low frequency distortions (wavelengths larger than 30 km), similar to that produced by residual orbital fringes due to orbit indetermination. On the contrary tropospheric disturbances are common even on a sub-kilometre scale, though most of their signal power is concentrated at low wavenumbers. In fact, the power spectrum of this kind of phenomena has already been studied in some detail. According to Williams et al. (1998) and recent results obtained using a multi-inteferogram by Ferretti et al. (1999a, 1999b), a sparse grid of ZPD estimates can strongly reduce the impact of this kind of phenomena on differential phase values. Whenever these kinds of measurements are not available or just a few of them can be identified in the area of interest, one can take advantage of standard ground meteorological data (P, T, H) in order to get a first order approximation of the atmospheric contribution.

Apart from the turbulent component, exhibiting the typical power law spectral behavior (Kolmogorov spectrum), InSAR data are sensitive to the mean meteorological conditions at the time of the acquisitions. This effect is more evident in mountainous areas where the atmospheric path delay is a function of the topographic profile, according to the different thickness of the troposphere.

Delacourt et al. (1997) applied a semiempirical approach developed for GPS in order to estimate and compensate several SAR interferograms of Etna for this kind of phenomena. Vertical refractive index gradient is modelled by a simple mathematical law, using two empirical parameters varying with local latitude and climate. The model predicts the atmospheric phase component at each pixel in the image using (1) a DEM of the area of interest and (2) ground meteorological data (P, T, H) acquired at a reference point of known co-ordinates.

As already pointed out in Williams et al. (1998) and Bevis et al. (1992), while surface measurements of T and P are adequate for predicting the hydrostatic component of the tropospheric delay, the predictive value of surface measurements of water vapour are very limited. Analysis of more than 70 radiosonde profiles gathered at Trapani meteorological station (200 km West of Etna) and the experimental values collected on Mt. Etna during GPS surveys on geodetic network, (Fig. 7) confirmed the highly unpredictable behavior of the humidity profile.

Notwithstanding these preliminary results, we estimated the atmospheric path delay relative to a dozen of SAR differential interferograms, using ground based meteorological data measured at Catania airport.

Different laws can be used to model the atmospheric water vapour as a function of the elevation. We found that the Saastamoinen model, used by Zebker et al. (1997) and only cited by Delacourt et al. (1997), gives better results than the semiempirical approach for the area of Mt. Etna. In fact the semiempirical model often underestimates the atmospheric component. This was clearly evident using low temporal baseline interferograms where phase contribution due to possible ground motions is negligible (Bonforte et al., 1999).

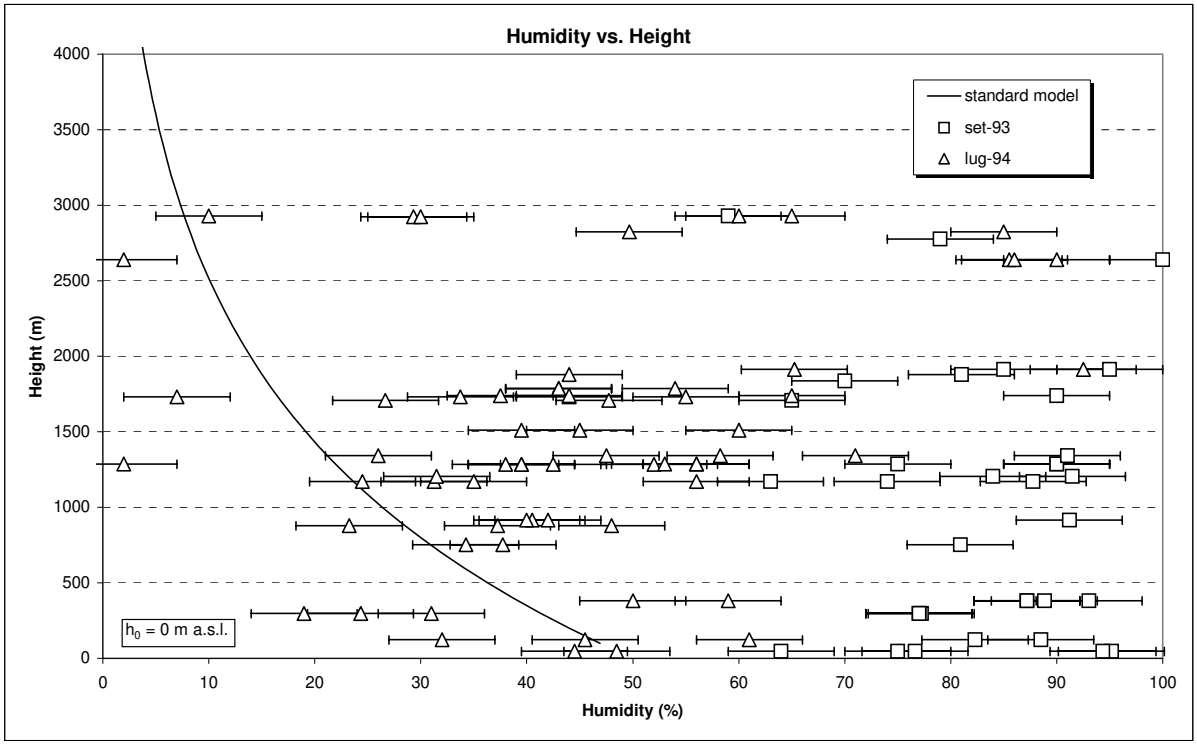

Figure 7: Example of humidity values measured on Mt. Etna during GPS surveys; the error bars derive from the experimental variations observed during the session (2-3 hours). The curve represents the standard model, function of the altitude, (Berg, 1948), computed assuming a value of the humidity H_0 = 50% at the reference level h_0. The experimental values are clearly randomly distributed.

An example of atmospheric compensation using the Saastamoinen model is reported in Figures 8 and 9. The differential interferogram relative to SAR images gathered on May, 28th 1997 and September, 9th 1997 shows an interesting fringe pattern that can be interpreted as due to an inflation of the volcanic edifice of more than 6 cm. The differential interferogram changes completely when the estimated atmospheric component is removed (Figure 9), since almost no fringe is visible. Though this is just a rough estimation of

the atmospheric component, it should be applied, at least to get an estimation of the reliability of the results: of course local atmospheric phenomena (clouds, fog, etc.) cannot be compensated, unless a multi-interferogram approach such as the "Permanent Scatterers Technique" is adopted (Ferretti et al. 1999b, 1999c).

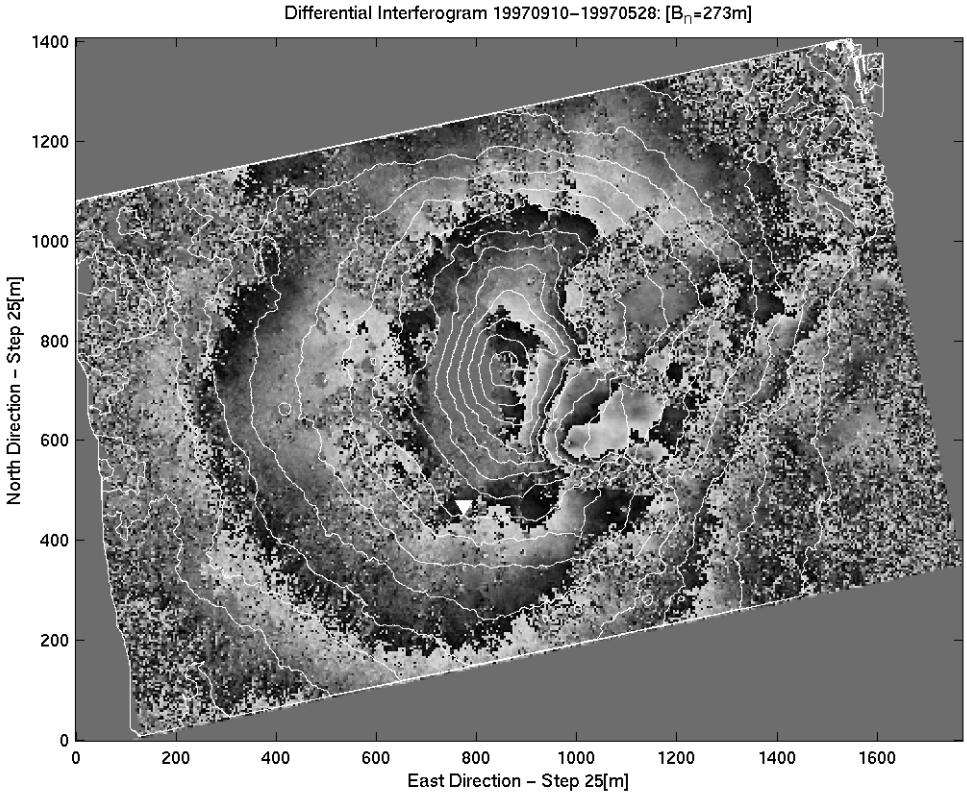

Figure 8: Differential Interferogram (19970910-19970528). The topographic contribution has been compensated using a precise DEM ($\sigma \sim 6$ *m*) of the area. To better identify the area, contour lines (200 *m* elevation step) of the local DEM are reported. The fringe pattern corresponds to a possible volcanic inflation. Each cycle corresponds to 2.8 cm of possible target motion in the direction of satellite line of sight. The white “down-triangle” corresponds to SLN station.

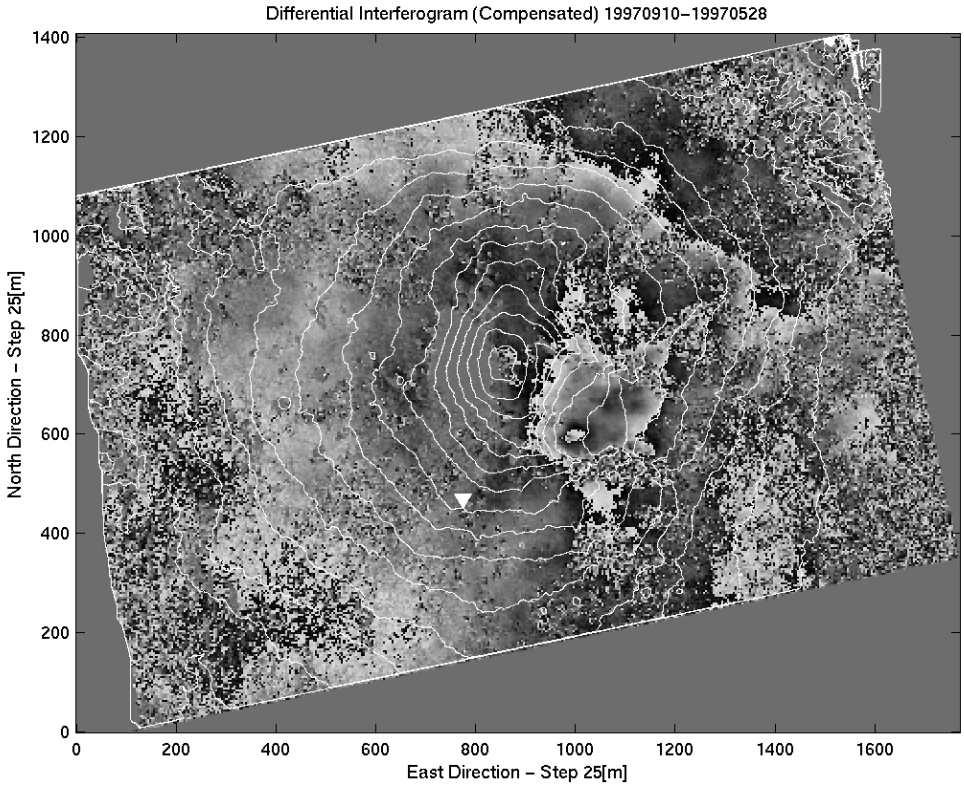

Figure 9: Differential Interferogram (19970910-19970528) compensated for the estimated atmospheric contribution. The atmospheric component superimposed on each SAR acquisition has been estimated using the Saastamoinen model (Zebker et al., 1997). Since wind direction is always West to East during the ERS SAR acquisitions, a turbulent atmospheric pattern is often visible on the East part of the mountain and cannot be compensated for using the simple meteorological model we have adopted.

Comparison of results and discussion

As far as the comparison between the results of Saastamoinen model-based correction of SAR interferograms and ZPD values estimated from GPS data is concerned, we selected the 8 ERS ascending acquisitions of our data set for which GPS ZPD data were available. Unfortunately, only 5 interferograms exhibited a satisfactory coherence level, so a statistical analysis proved to be impossible. Of course, a deeper and more extensive analysis will be necessary and these results should be considered preliminary. In any case, the differential interferograms always showed a number of fringes comparable with the estimated ZPD data (error always less than 1 cycle). Moreover, the ZPD estimated by GPS measurements appeared to be comparable with the values estimated from the Saastamoinen model and independent meteorological data, though this model always predicted higher values of the atmospheric delay.

Two examples of differential SAR interferograms are reported in Figures 10 and 11. It should be noted that, since wind direction is always West to East during the ERS ascending acquisitions (as usual on Mt. Etna), a turbulent atmospheric pattern is often visible on the East part of the mountain and cannot be compensated for using the simple meteorological model we have adopted. The corresponding estimated atmospheric delay between SLN and IIV, obtained from GPS measurements, is 0.24 ± 0.18 and 1.71 ± 0.19 cycles respectively (Fig. 4). In Figures 12 and 13 the atmospheric contribution relative to each differential interferogram estimated using the Saastamoinen model and ground based meteorological data is also

reported. The estimated atmospheric delay between SLN and IIV is now 0.7 and 2 cycles respectively. Of course, more severe atmospheric distortions have been observed when strong variations of the meteorological parameters have been reported. The resulting interferograms, compensated for the estimated atmospheric contribution, are reported in the Figures 14 and 15. The residuals now contain both the short wavelength errors of the model and the ground deformation component; however, even if it is impossible to discriminate between them with the available data, the latter seems not larger than 1-2 interferometric fringes.

These results confirmed both the suitability of the method based on the use of ground-based meteorological data and the comparability of their results with the evaluation of the tropospheric delay based on GPS data. This positive comparison suggests some applications of these results in view of a routinely use of the SAR in volcano monitoring systems. For instance, a GPS network installed in a volcanic area, for ground deformation monitoring purposes, could also produce a rapid estimation of ZPD to evaluate the effective suitability of the SAR images, before they are ordered and/or delivered (usually not before 2-3 weeks after the pass).

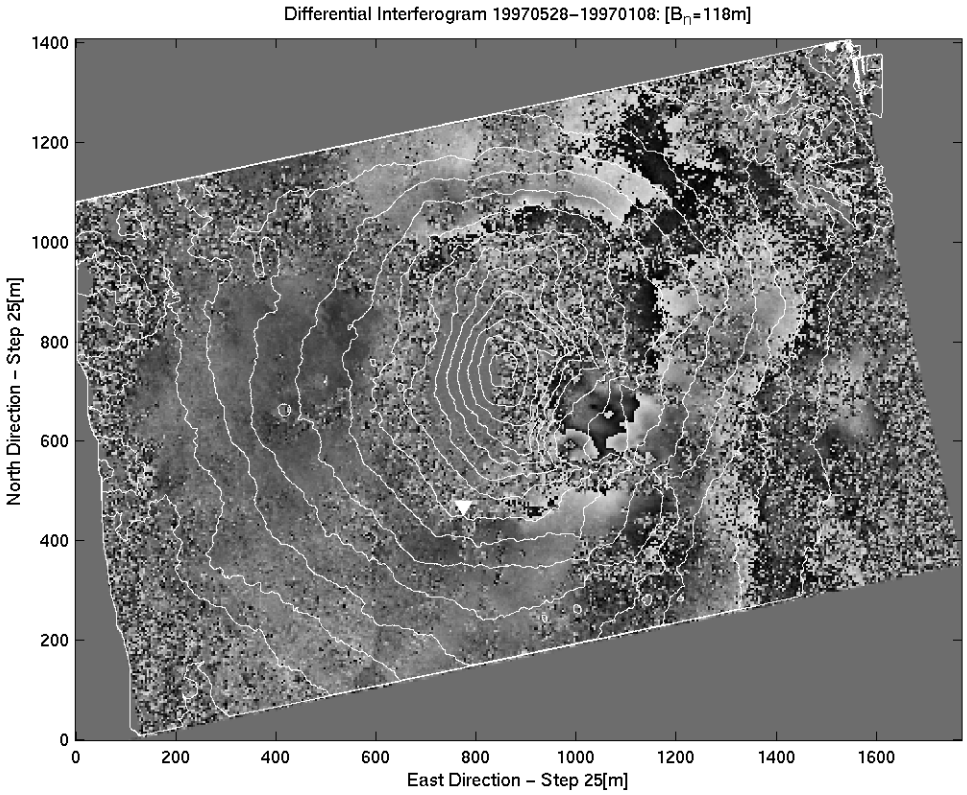

Figure 10: Etna differential interferogram (19970528-19970108).

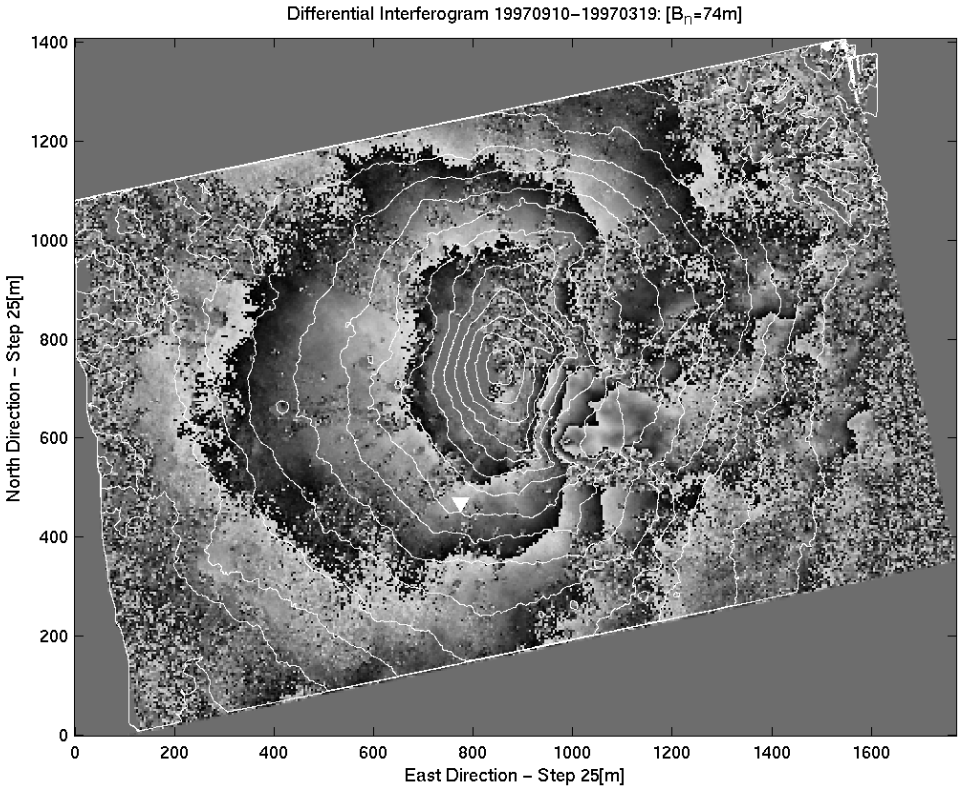

Figure 11: Etna differential interferogram (19970910-19970319).

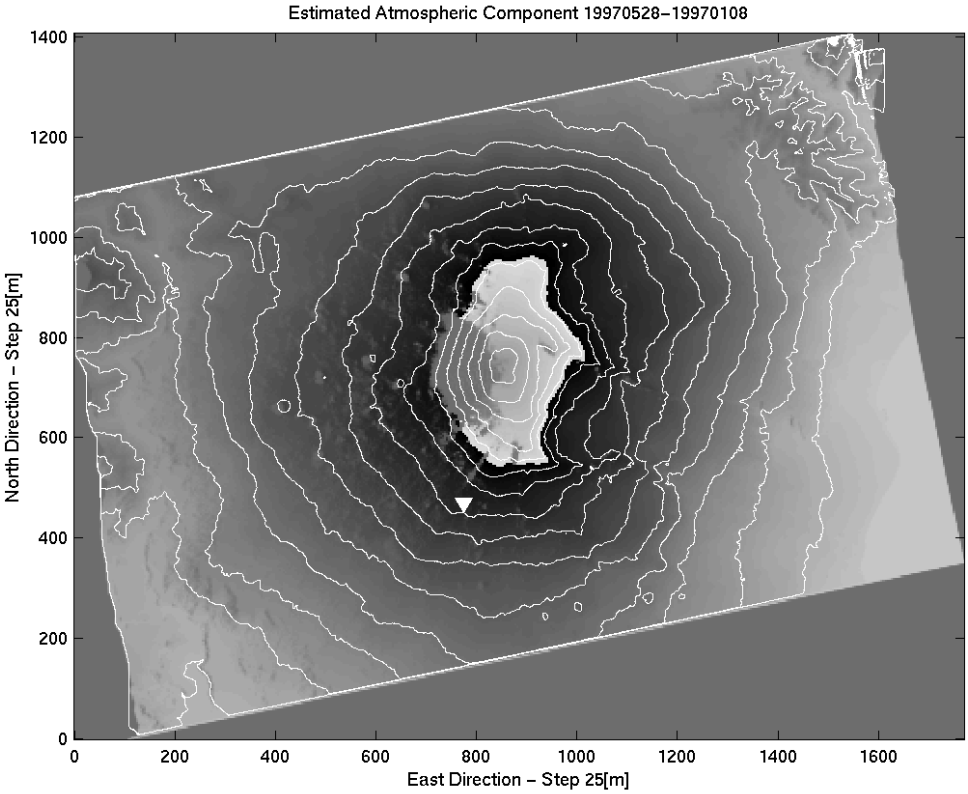

Figure 12: Estimated atmospheric phase component relative to 19970528-19970108 interferogram. Meteorological data: 19970528: P=1014 mbar, T=22.7 C, H=42%. 19970108: P=1014.4 mbar, T=7.4 C, H=91%.

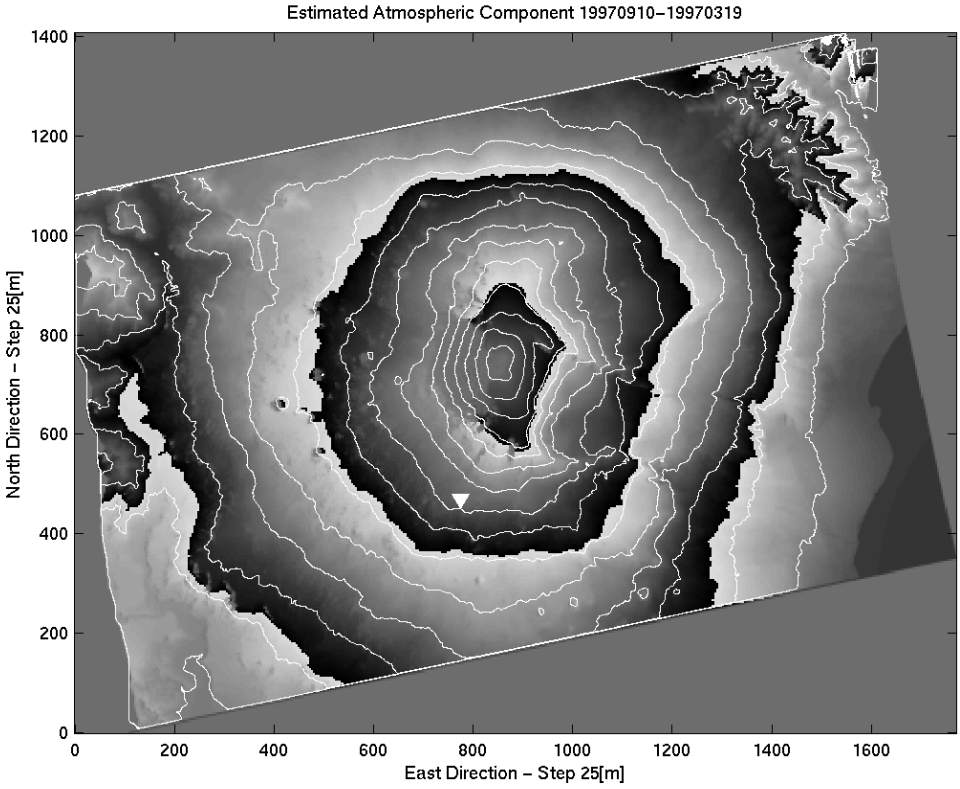

Figure 13: Estimated atmospheric phase component relative to 19970910-19970319 interferogram. Meteorological data: 19970910: P=1016 mbar, T=23.8 C, H=95%. 19970319: P=1008.7 mbar, T=13.2 C, H=84%.

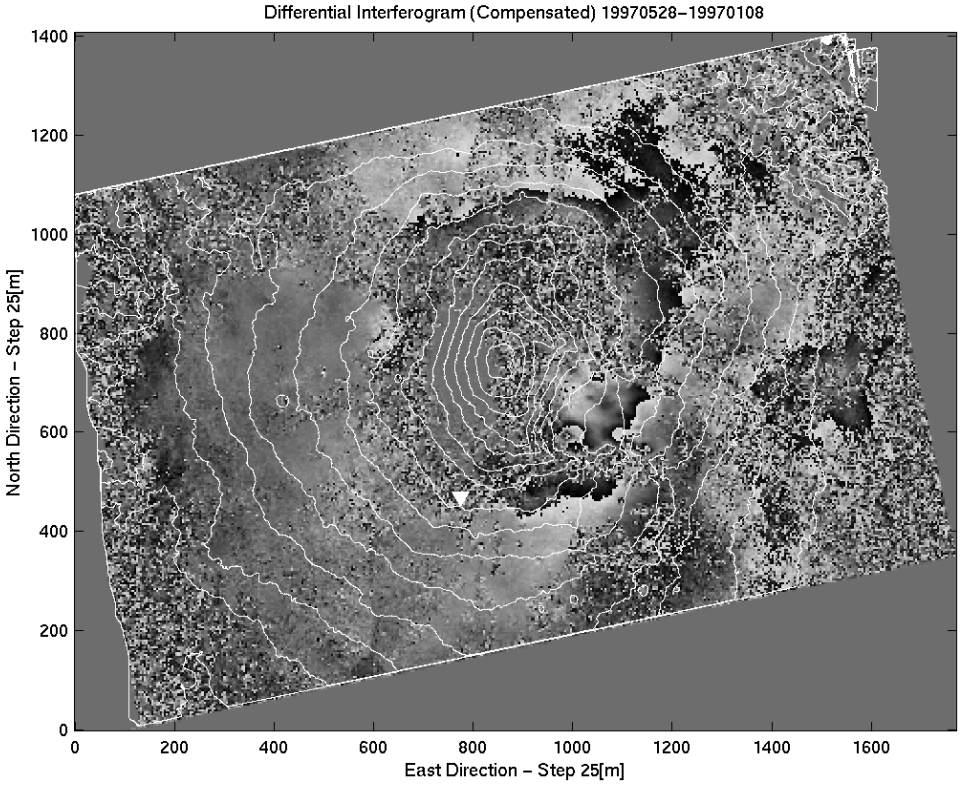

Figure 14: Differential Interferogram of Figure 10 compensated for the estimated atmospheric contribution.

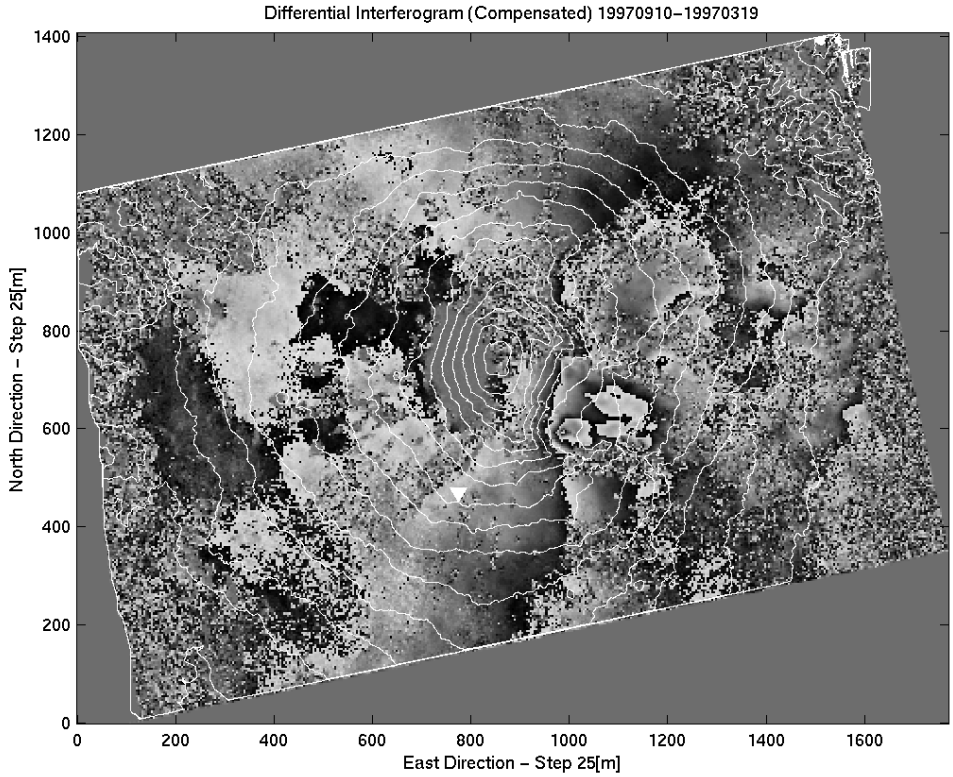

Figure 15: Differential Interferogram of Figure 11 compensated for the estimated atmospheric contribution.

However, this work highlights some critical points that may represent suggestions for further investigations. The first concerns the suitability of the standard models used to predict the vertical profile of P, T and H to describe the actual values and consequently the real ZPD profile. Apart from the difficulties relevant to the humidity, already mentioned above, the GPS results suggest that the vertical ZPD profile at Mt. Etna cannot be satisfactorily described by regular laws, since the higher part of the volcano shows a lower delay with respect the lower part. Furthermore, lateral heterogeneity of the troposphere, found close to the summit cones, could be related to the volcanic plume containing a large amount of volcanic gas (mainly water vapour) and ash. These observations from the results of GPS analysis highlight that the compensation methods of SAR interferograms, requiring ground-based meteorological data, might be improved by their calibration based on data from both the GPS network (ZPD) and more numerous meteorological stations (P, T, H). In the near future, Mt. Etna, like other volcanic areas, will be monitored by a dense permanent network of GPS stations that could provide the data required for the calibration. However, local small heterogeneity, such as that due to the atmospheric turbulence or volcanic activity, still represent a difficult task to be addressed with this kind of approach and probably more specific analysis will be required to overcome these particular problems. To this end, the multi-interferogram approach proposed by Ferretti et al. (1999b,1999c) seems to be very promising; the key point is the density of Permanent Scatterers in the area of interest. Future research efforts will be devoted to assess the suitability of this technique for volcano monitoring as an early warning system.

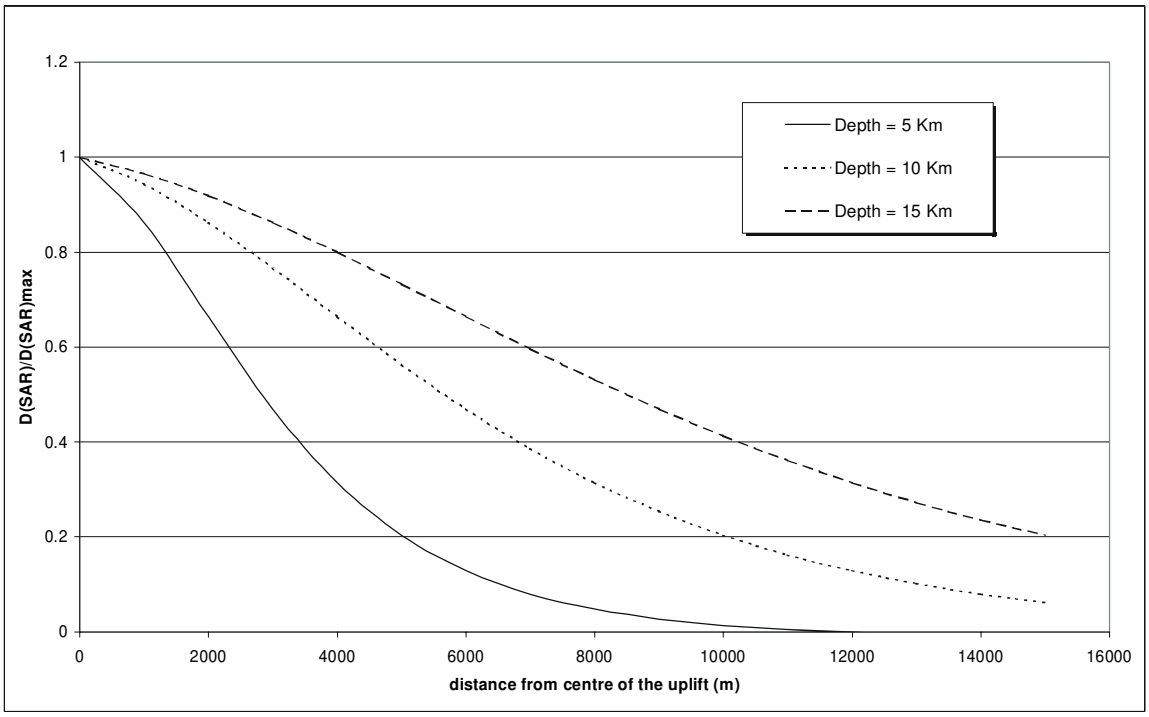

Figure 16: Example of deformation curves for the same Mogi (1958) source, located at different depth. The deformation are normalised with respect to the maximum of deformation, localised close to the vertical of the centre of the point source. The decay of the curves is higher for shallow sources than for the deep ones.

The impact of these results in the volcanological studies is relevant to founding the location of ground deformation sources. The large ZPD observed at lower altitudes could produce artificial interferometric fringes in these areas that might be viewed as indication of a large scale inflation or deflation of the volcano. Assuming a point source beneath the summit craters of the volcano, the inversion of these data brings about the source to be deeper than the true (Figure 16). This kind of inversion is very frequently performed in volcanology and we have recent examples of studies of ground deformation on Mt. Etna using SAR interferometry (Massonet et al., 1995; Lanari et al., 1998). It is singular that all the sources resulting from these studies are deeper than that obtained inverting other geodetic data (e.g. Bonaccorso, 1996; Nunnari & Puglisi, 1994b). The considerations here performed suggest that this misfit could be an effect of the atmosphere, though probably not totally due to it, as discussed in more detail by Puglisi et al. (1999).

Conclusions

Although the estimation of small ground deformations is still a challenge using a single SAR interferogram, our analysis shows that at least a first order approximation of the atmospheric component is possible using simple models. The estimation of the atmospheric delay (in particular the effects due to the lower troposphere) should be carried out especially when a strong topography characterises the image scene and SAR images have been acquired in different seasons, with notable variations in local meteorological parameters. To this end, ground based meteorological data and/or GPS measurements should be used whenever available. Moreover, the results of this preliminary study suggest a possible integration of GPS-based ZPD data with cheap and standard meteorological data, since the estimated atmospheric component

proved to be similar, even though not identical. Finally, an increase in the signal-to-noise ratio of the differential interferograms, by compensating the data with respect to the estimated atmospheric contributions, makes an easier and more reliable estimation of ground deformation using a multi-interferogram approach possible (Ferretti et al. 1999b). Of course, reduction in tropospheric disturbance increases with an increasing number of measurement points. The minimum number of data necessary to carry out the analysis and false alarm rates could be greatly reduced if more measurement points (GPS and/or meteorological stations) are available.

The examples reported in this paper show that the compensation of the atmospheric effects on the SAR interferograms produce a completely different pattern of the satellite-Earth range variation between the two passes, with respect to the original ones. This simple observation, highlights the importance to carefully address this effect in the ground deformation studies using SAR interferograms. Furthermore, the large effects expected - on the basis of GPS results - at lower altitudes, could bring about changes in the true ground deformation pattern that give rise to locate sources deeper than the actual ones when these data are inverted.

Acknowledgements

Thanks are due to B. Puglisi, O. Consoli and M. Bonaccorso, for the help in the GPS fieldwork and G. Rigamonti for his support in data processing. This research was funded in the frame of the 4th European Community program for Natural Hazard Reduction (MAD VIEWS project, ENV4-CT96-0294).

References

Berg H. (1948) - Algemeine Meteorologie. Dümmler Verlag, Bonn.

Beutler G., Gurtner W., Rothacher M., Wild U., Frei E. (1989) - Relative static positioning with the Global Positioning System: basic technical considerations. In "Global Positioning System: an overview". IAG Symp. 102, Springer-Verlag, Edinburgh, Aug. 7-8, 1989., 1-23.

Bevis M., Businger S., Herring T., Rocken C., Anthes R., Ware R. (1992) - GPS meteorology: remote sensing of atmospheric water vapor using Global Positioning System. J. Geoph. Res., 97, 15787-15801.

Bonaccorso A. (1996) - Dynamic inversion of ground deformation data for modelling volcanic sources (Etna 1991-1993). Geophys. Res. Lett., 23 (5), 451-454.

Bonforte A., Puglisi G., Ferretti A., Menegaz A., Prati C., Rocca F. (1999) – Modelli atmosferici per il controllo di movimenti dell'Etna. Alta Frequenza – Rivista di Elettronica, 11, 4, 34-39.

Briole P., Gaulon R., Nunnari G., Puglisi G., Ruegg J.C. (1992) - Measurements of ground movement on Mount Etna, Sicily: a systematic plan to record different temporal and spatial components of ground movement associated with active volcanism. IAVCEI Proc. Volc., P. Gasparini, R. Scarpa, K. Aki eds., Springer-Verlag, Berlin, 3, 120-129.

Briole P., Massonnet D., Delacourt C. (1997) - Post-eruptive deformation associated with the 1986-87 and 1989 lava flows of Etna detected by radar interferometry. Geophys. Res. Lett., 24, 37-40.

Delacourt C., Briole P., Achache J. (1997) - Tropospheric correction of the SAR interferograms with strong topography. Application to Etna. Geophys. Res. Lett., 25, 15, 2849-2852.

Essen L. and Froome K.D. (1951) - The refractive indices and dielectric constants of air and its principal constituents at 24000 Mc/s. Proc. of Phys. Soc., 64(B), 862-875.

Ferretti A., Prati C., Rocca F. (1999a) - Multibaseline InSAR DEM reconstruction: the wavelet approach. IEEE Trans. Geosc. And Rem. Sens., 37(2), 705-715.

Ferretti A., Prati C., Rocca F. (1999b) - Permanent Scatterers in SAR interferometry. Submitted to IEEE Trans. Geosc. And Rem. Sens., June 1999.

Ferretti A. Prati. C., Rocca F. (1999c) - Permanent Scatterers in SAR Interferometry. Proc. Int. Geoscience and Rem.Sensing Symposium (IGARSS), Hamburg, Germany, 1999.

Goad C.C. and Goodman L. (1974) - *A Modified Hopfield Tropospheric Refraction Correction Model*. In "Proceeding of the Fall Annual Meeting of the Ametican Geophysical Union", San Francisco, California, December 12-17.

Lanari R., Lundgren P., Sansosti E. (1998) - Dynamic deformation of Etna volcano observed by satellite radar interferometry. Geophys. Res. Lett., 25, 1541-1544.

Mogi K (1958) - Relation between the Eruptions of Various Volcanoes and the Deformations of the Ground Surfaces around them. Bull. Earth Res. Inst. 36: 99-134.

Massonnet D., Briole P., Arnaud A. (1995) - Deflation of Mount Etna monitored by spaceborne radar interferometry. Nature, 375, 567-570.

Massonnet D., Rabaute T. (1993). Radar interferometry: limits and potential. IEEE Trans. Geosc. And Rem. Sens., 31, 455-464.

Nunnari G., Puglisi G., 1994a: The Global Positioning System as a useful technique for measuring ground deformations in volcanic areas. J. Volcan. Geoth. Res., 61, 3/4, 267-280.

Nunnari G, Puglisi G (1994b) - Ground deformation studies during the 1991-1993 Etna eruption using GPS data. Acta Vulcanologica, 4, 101-107.

Puglisi G., Bonaccorso M., Bonforte A., Campisi O., Consoli O., Maugeri S.R., Nunnari G., Puglisi B., Rossi M., Velardita R. (1998) - 1993-1995 GPS measurements on Mt. Etna: improvements in network configuration and surveying techniques. Acta Vulcanologica, 10(1), 158-169.

Puglisi G., Bonforte A., Maugeri S.R. (1999) - Ground deformation patterns on Mt. Etna, between 1992 and 1994, inferred from GPS data. Bull. Volcanol., in press.

Rosen P.A., Hensley S., Zebker H.A., Webb F.H., Fielding E.J. (1996) - Surface deformation and coherence measurements on Kilawea Volcano, Hawaii, from SIR-C radar interferometry. J. Geoph. Res., 101, E10, 23109-23125.

Rothacher M., Beutler B., Gurtner W., Geiger A., Kahle H.G. and Schneider D. (1986) - *The Swiss 1985 GPS Campaign*. In Proceeding of the Fourth International Symposium on Satellite Positioning, 2, 979-991, Austin, Texsas.

Rothacher M. and Mervart L. Eds. (1996) - BERNESE GPS software. Astronomical Institute University of Berne.

Saastamoinen I.I. (1973) - Contribution to the theory of atmospheric refraction. Bulletin Géodésique, 107, 13-34.

Wells D.E. (1974) - Doppler Satellite Control. Dep of Surveying Eng., Univ. of New Brunswich, Fredericton, N.B.

Williams S., Boch Y., Fang P. (1998) - Integrated satellite interferometry: Tropospheric noise, GPS estimates and implications for interferometric synthetic aperure radar products. J. Geoph. Res., 103, B11, 27051-27067.

Zebker H. A., Rosen P. A., Hensley S. (1997) - Atmospheric effects in interferometric synthetic aperture radar surface deformation and topographic maps. J. Geophys. Res., 102, 7547-7563.